

Cp*Fe(Me₂PCH₂CH₂PMe₂)(CHO): Hydride Shuttle Reactivity of a Thermally Stable Formyl Complex

Joshua S. Sapsford,^a Sarah J. Gates,^a Laurence R. Doyle,^b Russell A. Taylor,^{c,d} Silvia Díez-González,^{a,*} Andrew E. Ashley^{a,*}

^a Department of Chemistry, Molecular Sciences Research Hub, Imperial College London, Wood Lane, London, W12 0BZ, UK.

^b School of Chemistry, University of Manchester, Manchester, M13 9PL, UK.

^c BP plc, c/o BP Chemicals Limited, Saltend, Hull, HU12 8DS, UK.

^d Current address: Department of Chemistry, Durham University, South Road, Durham, DU1 3LE, UK.

Abstract

[Cp*Fe(Me₂PCH₂CH₂PMe₂)(CO)]⁺ [BARF₂₄]⁻ has been synthesised and characterised using single crystal X-ray diffraction, NMR and IR spectroscopies. Reduction of the CO ligand using Na[Et₃BH] produces the corresponding neutral formyl complex Cp*Fe(Me₂PCH₂CH₂PMe₂)(CHO), that is very thermally stable, and which is attributed to the electron-releasing properties of the spectator ligands. This compound is a potent hydride donor which exists in equilibrium with [Et₃BH]⁻, Et₃B, and the structural isomer (η⁴-C₅Me₅H)Cp*Fe(Me₂PCH₂CH₂PMe₂)(CO), resulting from reversible hydride migration to the Cp* ligand.

Introduction

As global energy demands increase, it is becoming increasingly necessary to have secure stable, renewable feedstocks for fuel generation. Syngas (CO + H₂ mixtures) can be made from natural gas, coal, or biomass.[1] One of the most important uses of syngas is the Fischer-Tropsch (FT) process, whereby liquid fuels can be synthesized via the reductive polymerisation of CO under elevated temperatures and pressures, commonly employing Fe or Co catalysts. FT processes typically use heterogeneous catalysts, where continuous processes, scalability, and readily separable components are preferred. However, homogeneous alternatives can offer greater selectivity in catalysis, milder reaction conditions and, crucially, a better understanding of the mechanism.[2]

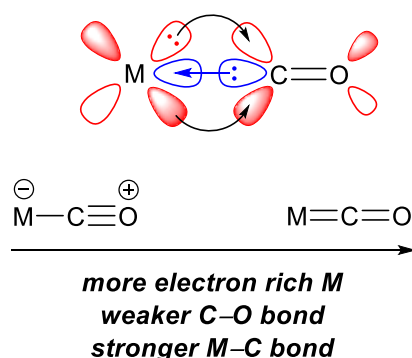
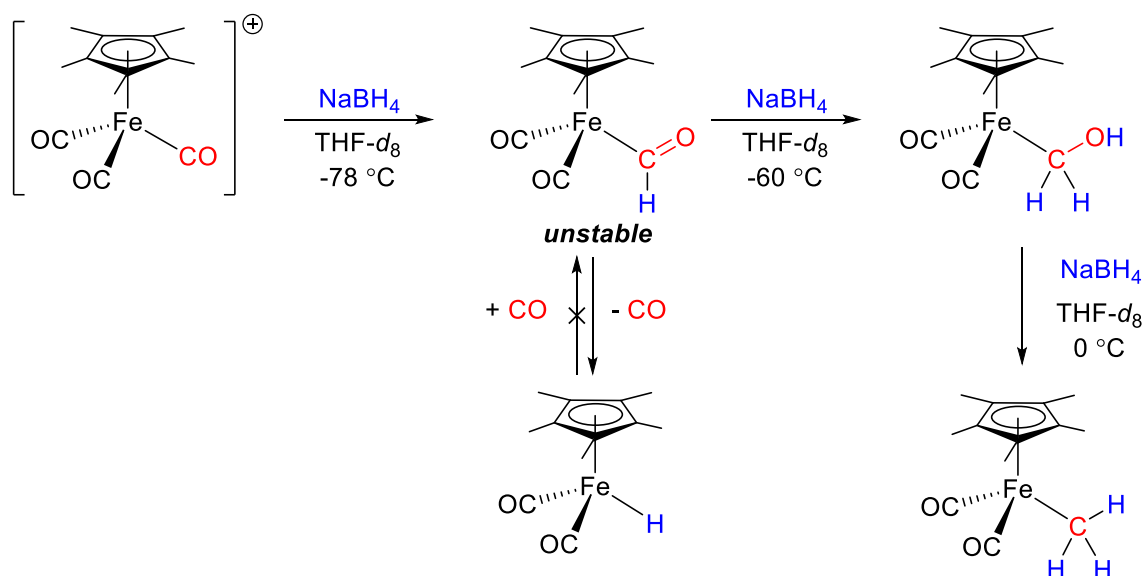


Figure 1. Transition metal carbonyl bonding: (1) electron density from a filled σ -symmetry orbital on the CO ligand is donated to an empty metal-based σ -orbital (blue); (2) electron density from filled metal π -symmetry orbitals is back-donated into an empty π^* C–O orbital (red). The latter dominates and predominantly affects the bond strengths of the M–C and C–O bonds. M = transition metal.

Homogeneous FT studies have focused on using transition metal CO complexes. The bonding interaction between the metal and CO ligand is well established: the lone pair on C is donated into a vacant d orbital, while a filled d orbital on the metal donates back into the vacant C–O π^* orbital (Figure 1). The relative contribution of these two effects depends on the electron density at the metal, with a more electron rich centre translating to stronger back bonding, which in turn increases the M–C bond order with concomitant decrease of the C–O bond strength.



Scheme 1. Previously reported stepwise reductions of $[\text{Cp}^*\text{Fe}(\text{CO})_3]^+$ with NaBH_4 . The intended product is where the CO ligand is reduced to CH_3 . A competing pathway where the formyl complex irreversibly decarbonylates is also shown.

The migratory insertion of the hydride ligand into the M–CO bond within an H–M–CO moiety to generate a formyl species M–CHO, is generally considered to be a thermodynamically unviable initial step of CO reduction.[3,4] Some strategies have employed oxophilic transition metals that coordinate strongly to the the formyl O atom, which stabilises the oxycarbene resonance form (Figure 2) and can drive overall migratory insertion of CO into an M–H bond.[5,6] However, the majority of previous attempts to hydrogenate a CO ligand have targeted the nucleophilic attack of hydride upon M–CO using external main-group reductants.[7] For example, Astruc *et al.* demonstrated the stepwise delivery of hydride from NaBH_4 to CO utilising $[\text{Fp}^*(\text{CO})]^+$ ($\text{Fp}^* = [\text{Cp}^*\text{Fe}(\text{CO})_2]$; $\text{Cp}^* = \eta^5\text{-C}_5\text{Me}_5$; Scheme 1), which proceeded via the key $\text{Fp}^*(\text{CHO})$, $\text{Fp}^*(\text{CH}_2\text{OH})$ and $\text{Fp}^*(\text{CH}_3)$ intermediates. The use of NaBH_4 is notable here since, in addition to being a potent source of H^- , it also generates BH_3 under the reaction conditions which can coordinate and polarise the CHO ligand, rendering $\text{Fp}^*(\text{CHO})$ susceptible to further reduction. Competing with this productive pathway is the decarbonylation of $\text{Fp}^*(\text{CHO})$ to form Fp^*H and CO; since the reverse of this reaction is energetically unfeasible, this represents an irreversible side reaction and hence a major barrier to achieving catalysis with such systems.[8]

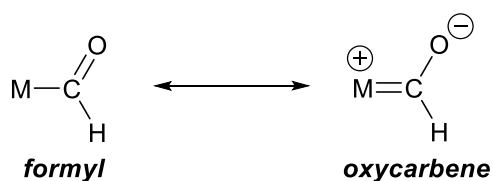


Figure 2. Canonical forms of a transition metal formyl complex.

To facilitate strengthening of the metal-formyl bond, a more stable complex would be one in which the oxycarbene canonical form dominates, which has a stronger M–C bond. A potential route to suppressing decarbonylation in the parent $[\text{Cp}^*\text{Fe}(\text{CO})_3]^+$ system therefore would be to increase the electron density of the Fe metal centre through the use of electron-donating co-ligands, thereby augmenting back-bonding and the Fe-CHO bond order. Furthermore, incorporating strongly chelating ligands into the coordination sphere of Fe, such as bidentate phosphines, would theoretically inhibit the formation of intermediates with lower coordinate numbers and lower valence-electron count (e.g. 16), which can promote decarbonylation. The use of *bis*phosphines as ancillary ligands in Fe-mediated CO reduction chemistry remains relatively unexplored. Initial investigations utilised *bis*(diphenylphosphino)ethane (dppe) e.g. $[\text{CpFe}(\text{dppe})(\text{CO})]^+$, whereupon dissociation of a phosphine arm occurred readily upon hydride attack from an external reductant, forming an Fe carbonyl hydride instead of Fe-CHO; analogous reactivity was observed with monodentate phosphines (e.g. PMe_3 , PPh_3) in $[\text{CpFe}(\text{PR}_3)(\text{CO})_2]^+$. [9] Davies *et al.* documented the reactivity between LiAlH_4 and $[\text{CpFe}(\text{dmpe})(\text{CO})]^+$, that incorporates the strongly electron-donating ligand dmpe [dmpe = 1,2-bis(dimethylphosphino)ethane, $\text{Me}_2\text{PCH}_2\text{CH}_2\text{PMe}_2$], which afforded $\text{CpFe}(\text{dmpe})(\text{CH}_3)$; in contrast with dppe, it was postulated that dmpe coordinates sufficiently strongly to stabilise the incipient formyl enough to enable further reduction to the alkyl complex. [10,11]

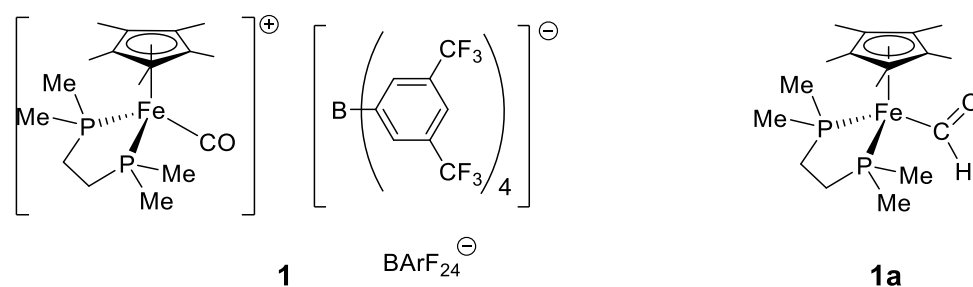


Figure 3. Synthetic targets of this study: $[\text{Cp}^*\text{Fe}(\text{dmpe})(\text{CO})]^+[\text{BARF}_{24}]^-$ (**1**) and $\text{Cp}^*\text{Fe}(\text{dmpe})(\text{CHO})$ (**1a**); dmpe = $\kappa^2\text{-Me}_2\text{PCH}_2\text{CH}_2\text{PMe}_2$.

It is apparent that increasing the electron density at the metal centre can impart a considerably greater stability to Fe formyl complexes, which aids in studies of their reactivity. To date, however, the electron donor ‘limit’ in these Fe-CO reduction systems has been reached using a bidentate dialkylphosphine and Cp ancillary ligand set. We have recently been investigating the reduction of the N_2 ligand by Fe compounds which are supported by 1,2-*bis*(dialkylphosphino)ethane ligands, where the electron-rich nature of the latter plays an important role in stabilising intermediates in catalytic cycles. [12,13] We became interested in expanding our interests to investigate the hydride-reduction chemistry of the CO ligand, with which N_2 is isoelectronic, in Fe complexes incorporating *both* the strongly electron-donating pentamethylcyclopentadienyl (Cp^*) and dmpe ligand. Accordingly, we targeted the cationic carbonyl fragment $[\text{Cp}^*\text{Fe}(\text{dmpe})(\text{CO})]^+$ with the aim of facilitating the formation, and increasing the stability, of a resultant formyl complex (see Figure 3 for synthetic targets of this study).

Experimental section

General experimental considerations

Unless stated otherwise, all reactions and compounds were manipulated under N₂ using standard Schlenk techniques on a dual manifold vacuum/inert gas line or in a MBraun Labmaster DP glovebox. All glassware was heated to 180 °C overnight before use. Solvents and solutions were transferred between vessels using a positive pressure of N₂ through stainless steel cannulae, or via plastic syringes for smaller volumes (< 20 mL). Filtrations were performed using either glassware fitted with a sintered glass frit, or by using modified stainless steel cannulae fitted with a glass microfibre filter.

The 1,2-*bis*(dialkylphosphino)ethane ligand dmpe was prepared according to our previously published procedure.[14] Cp*Fe(CO)₂Cl (Fp*Cl) was synthesised according to a published procedure.[15]

Toluene, pentane and chloroform were dried using an Innovative Technology Pure Solv SPS-400; diethyl ether and THF were distilled from purple Na/benzophenone diketyl. Toluene, pentane and diethyl ether were stored over a K mirror; chloroform and THF were stored over 4 Å molecular sieves. CDCl₃ and CD₂Cl₂ were freeze-pump-thaw degassed and stored over 4 Å molecular sieves.

NMR spectra were recorded using Bruker AV-400 (400 MHz), DRX-400 (400 MHz) and AV-500 (500 MHz) spectrometers at room temperature unless otherwise stated. Chemical shifts, δ , are reported in parts per million (ppm) downfield from the reference nucleus. ¹H and ¹³C{¹H} NMR chemical shifts are reported relative to Me₄Si and referenced to the residual *proteo*-signal of the deuterated solvents used. ³¹P{¹H} NMR spectra are referenced externally to 85% H₃PO_{4(aq)}.

Elemental analysis was conducted by Mr S. Boyer of the London Metropolitan University.

IR spectroscopic data collection

IR spectra were recorded on a Perkin Elmer GX FT-IR spectrometer (range 4000-400 cm⁻¹, resolution 0.5 cm⁻¹) as solutions. All air sensitive samples were loaded into an air-tight Specac[®] Omni Cell[™] at *ca.* 0.01 M concentrations using a syringe in a glovebox.

X-ray diffraction analysis

A suitable crystal was selected and mounted on a glass fibre with polyfluorether oil on an Oxford Diffraction Xcalibur diffractometer. The crystal was kept at 173.00(14) K during data collection. Using Olex2,[16] the structure was solved with the olex2.solve[17] structure solution program using Charge Flipping and refined with the ShelXL[18] refinement package using Least Squares minimisation.

Synthesis of [Cp*Fe(dmpe)(CO)][BARF₂₄] (1)

In a sealed Schlenk bomb, 1,2-bis(dimethylphosphino)ethane (0.21 g, 1.4 mmol) and Cp*Fe(CO)₂Cl (0.40 g, 1.4 mmol) were combined in toluene (20 mL), whereupon there was an immediate colour change from red to yellow. The solution was refluxed overnight, after which the volatiles were removed *in vacuo* to afford yellow solids. These were dissolved in THF (20 mL) and NaBARF₂₄ (1.26 g, 1.42 mmol) was added. The solution was stirred vigorously for 1 h at RT and filtered. The volatiles were subsequently removed *in vacuo* to afford a yellow solid. The crude solid was dissolved in CHCl₃,

filtered and the volatiles again removed *in vacuo*. Recrystallisation of the solid from a layering a saturated Et₂O solution with pentane afforded **1** (1.00 g, 0.81 mmol, 57%) as yellow-orange crystals.

¹H NMR (400 MHz, CDCl₃) δ: 7.70 (s, 8H, B-(*m*Ar-*H*)₄), 7.53 (s, 4H, B-(*p*Ar-*H*)₄), 1.68-1.86 (s, 15H, C₅(CH₃)₅), 1.68-1.86 (m, 4H, -PCH₂CH₂P-), 1.47-1.54 (m, 6H, -P(CH₃)₂), 1.34-1.40 (m, 6H, -P(CH₃)₂).

³¹P{¹H} NMR (162 MHz, CDCl₃) δ: 70.2.

¹³C{¹H} NMR (101 MHz, CDCl₃) δ: 215.0 (CO), 161.8, 134.7, 129.1, 125.6, 123.4, 121.3, 117.5, 94.4, 29.9, 18.0, 16.1, 10.0.

MS (ES⁺, *m/z*): for [C₁₇H₃₁FeOP₂]⁺ calcd: 369.22. Found 369.00.

IR (CD₂Cl₂, cm⁻¹): ν/CO 1947.

Anal. Calcd. for C₄₉H₄₃BF₂₄FeOP₂: C, 47.47; H, 3.52. Found: C, 47.68; H, 3.82.

Isotopic labelling of **1** with ¹³CO

1 (12.5 mg, 0.01 mmol) was dissolved in THF-*d*₈ in an NMR tube fitted with a J. Young's valve. The solution was freeze-pump-thaw degassed and ¹³CO (1 bar) was admitted while the solution was at –196 °C (equivalent to approximately 4 bar at room temperature). The solution was then irradiated with UV light (254 nm) for 5 h, with the extent of isotopic substitution periodically followed by ¹³C NMR spectroscopy. The resulting labelled solution containing **1**-¹³CO was subsequently used in the reduction procedure described below.

Reduction of **1** with Na[Et₃BH]

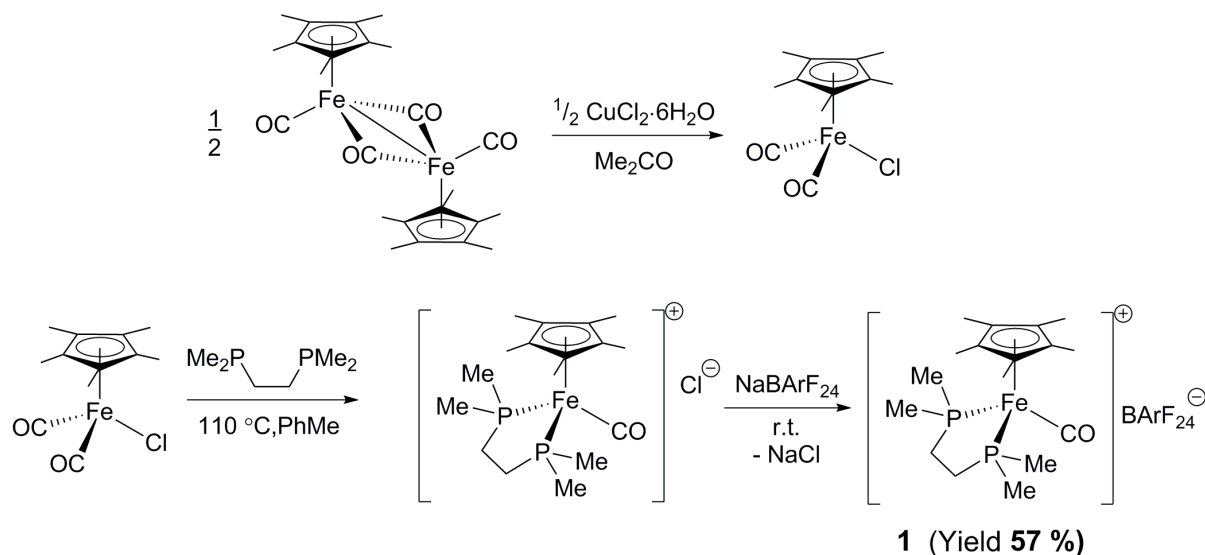
1 (12.5 mg, 0.01 mmol) and Na[Et₃BH] (10.0 μL, 1.0 M in THF, 0.01 mmol) were combined in *proteo*-THF (0.4 mL) in an NMR tube fitted with a J. Young's valve, to which was also added a capillary insert containing PPh₃ in C₆D₆ (to provide a lock and reference).

Complete conversion of **1** to **1b**

To a solution of **1** (12.5 mg, 0.01 mmol) in THF-*d*₈ (0.4 mL) in an NMR tube fitted with a J. Young's valve was added BEt₃ (30.0 μL, 1.0 M in hexanes, 0.03 mmol) and NaH (2.4 mg, 0.1 mmol). the tube was sonicated and shaken twice over a 2 h period, whereupon the only observable ³¹P NMR resonance (δ = 58.6 ppm) being that for **1b**.

Results and discussion

Synthesis of $[\text{Cp}^*\text{Fe}(\text{dmpe})(\text{CO})][\text{BArF}_{24}]$ (**1**)



Scheme 2. Synthetic route to compound **1**.

Previously reported synthetic routes to $[\text{Cp}^*\text{Fe}(\text{bisphosphine})(\text{CO})]^+$ species involve multiple low-yielding steps via photolysis and salt metathesis of parent $\text{Cp}^*\text{Fe}(\text{bisphosphine})\text{Cl}$ compounds under a CO atmosphere.[19] Our protocol, which is considerably better-yielding and less time-consuming, involved initial preparation of $\text{Cp}^*\text{Fe}(\text{CO})_2\text{Cl}$ (Fp^*Cl) via the clean oxidation of $[\text{Cp}^*\text{Fe}(\text{CO})_2]_2$ (Fp^*_2) with CuCl_2 , according to the method of Dias *et al* (see Scheme 2).[15] If a one-pot reaction of $\text{Cp}^*\text{Fe}(\text{CO})_2\text{Cl}$, dmpe, and $\text{Na}[\text{BArF}_{24}]$ is used to try and access $[\text{Cp}^*\text{Fe}(\text{bisphosphine})(\text{CO})][\text{BArF}_{24}]$ (**1**), a significant amount of $[\text{Cp}^*\text{Fe}(\kappa^1\text{-Me}_2\text{PCH}_2\text{CH}_2\text{PMe}_2)(\text{CO})_2]^+\text{BArF}_{24}^-$ contaminant is formed; this issue may be conveniently circumvented by ensuring full coordination of dmpe first via precipitation of the halide salt $[\text{Cp}^*\text{Fe}(\kappa^2\text{-dmpe})(\text{CO})]^+\text{Cl}^-$, and subsequent isolation of this material prior to chloride metathesis with NaBArF_{24} .

Characterisation of **1**

A single crystal of **1** suitable for X-ray diffraction studies was obtained through slow diffusion of pentane into a layered Et_2O solution of **1** at room temperature. The crystallographic data (deposited in the Cambridge Structural Database, CCDC 1877444) were collected, refined, and solved as the expected structure shown in Figure 4, with selected bond lengths shown in Table 1.

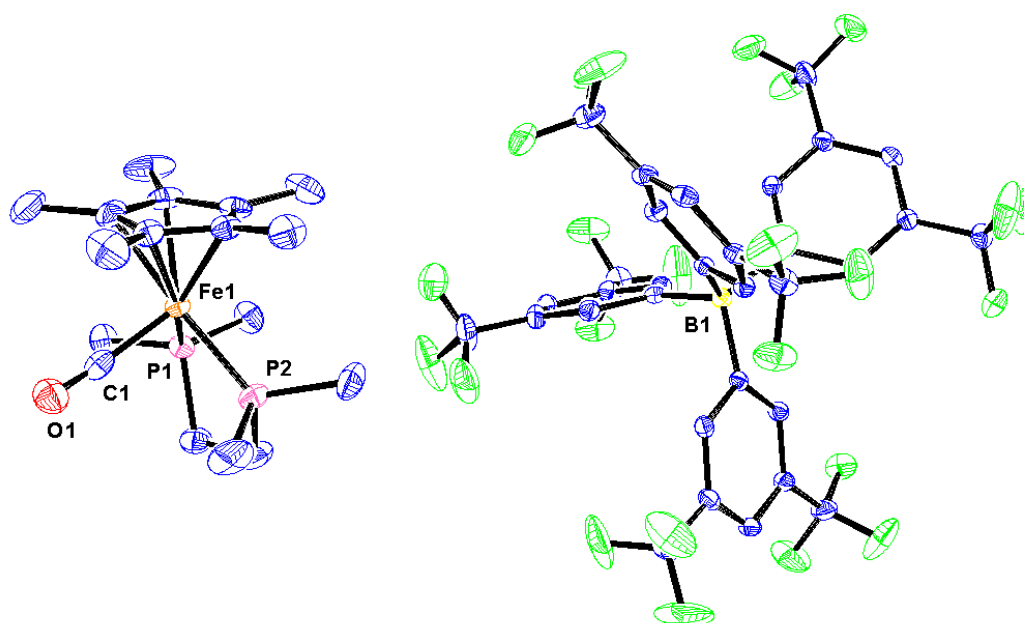


Figure 4. ORTEP diagram of the atoms in the unit cell of **1**; H atoms have been omitted for clarity. Anisotropic displacement ellipsoids are pictured at 30% probability (Fe atom orange, O atom red, C atoms blue, P atoms pink, B atom yellow, F atoms green).

| Bond | Bond length (Å) |
|--------|-----------------|
| C1–O1 | 1.052 (7) |
| Fe1–C1 | 1.794 (5) |
| Fe1–P1 | 2.200 (1) |
| Fe1–P2 | 2.203 (1) |

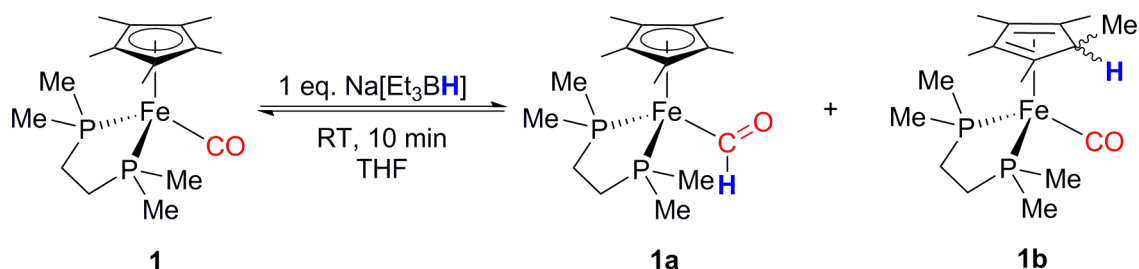
Table 1. Selected bond lengths from the solid-state structure of **1**.

| Compound | ν_{CO} (CH_2Cl_2 ; cm^{-1}) | Reference |
|--|---|-----------|
| $[\text{Cp}^*\text{Fe}(\text{CO})_3]^+[\text{PF}_6]^-$ | 2130, 2078 | [20] |
| $[\text{Cp}^*\text{Fe}(n\text{Bu}_3\text{P})(\text{CO})_2]^+[\text{PF}_6]^-$ | 2040, 1965 | [9] |
| 1 | 1947 | this work |

Table 2. IR C–O stretching frequencies for relevant Cp^*Fe cations.

The C–O bond strengths were also probed using IR spectroscopy (see Table 2). As anticipated, ν_{CO} is considerably lower for **1** vs the related compounds $[\text{Cp}^*\text{Fe}(\text{CO})_3]^+$ and $[\text{Cp}^*\text{Fe}(n\text{Bu}_3\text{P})(\text{CO})_2]^+$. Even when appreciating the different molecular symmetries, this shows that dmpe exerts a considerably greater electron-donating effect at the Fe centre (thus promoting enhanced back-bonding) than CO or a monodentate trialkylphosphine ligand.

Reduction studies



Scheme 3. Stoichiometric reduction of **1** with Na[Et₃BH], showing the products **1a** and **1b** as structural isomers.

Attempts to reduce either **1** using NaBH₄, even under heating to 60°C in THF, were not successful which indicates that the hydride ion accepting ability of this more electron-rich complex is notably poorer than [Cp*Fe(CO)₃]⁺. Gratifyingly though, addition of 1 equivalent of the more potent hydride donor Na[Et₃BH] led to rapid reduction of **1** to the corresponding formyl complex Cp*Fe(dmpe)(CHO) **1a** (Scheme 3). **1a** shows a diagnostic formyl CHO triplet in its ¹H NMR spectrum [δ (ppm) = 13.10; ³J (HP) = 7 Hz], which compares well with ³J (HP) ~ 5 Hz found for the related Fe-phosphine-formyl complexes Cp*Fe(CO)(CHO)(PR₃) (R = Me, Ph, *n*Bu), reported by Astruc *et al.*[9] The ³¹P{¹H} NMR spectrum for this reaction shows two distinct product resonances, in addition to starting **1**, however, revealing that the conversion to **1a** is incomplete. ¹H–³¹P NMR correlation spectroscopy (HMBC) confirmed the ³¹P NMR resonance attributable to the formyl product through observation of ¹H–³¹P coupling [³¹P: δ (ppm) = 85.4 (**1a**)], which is approximately 15 ppm downfield of the respective starting carbonyl complex [³¹P: δ (ppm) = 70.2(**1**)]. The third unknown resonance [³¹P: δ (ppm) = 58.6 (**1b**)] could be a product of further reduction, possibly containing an oxymethylene (–CH₂O–) moiety from further H[–] attack upon the formyl complex. Of note, ¹H NMR analysis of the reaction mixture did not show diagnostic signals which would constitute evidence for Fe–CH₃ or Fe–H species (i.e. δ < 0 ppm) comparable with those reported by Astruc and co-workers in related studies on [Cp*Fe(CO)₃]⁺.

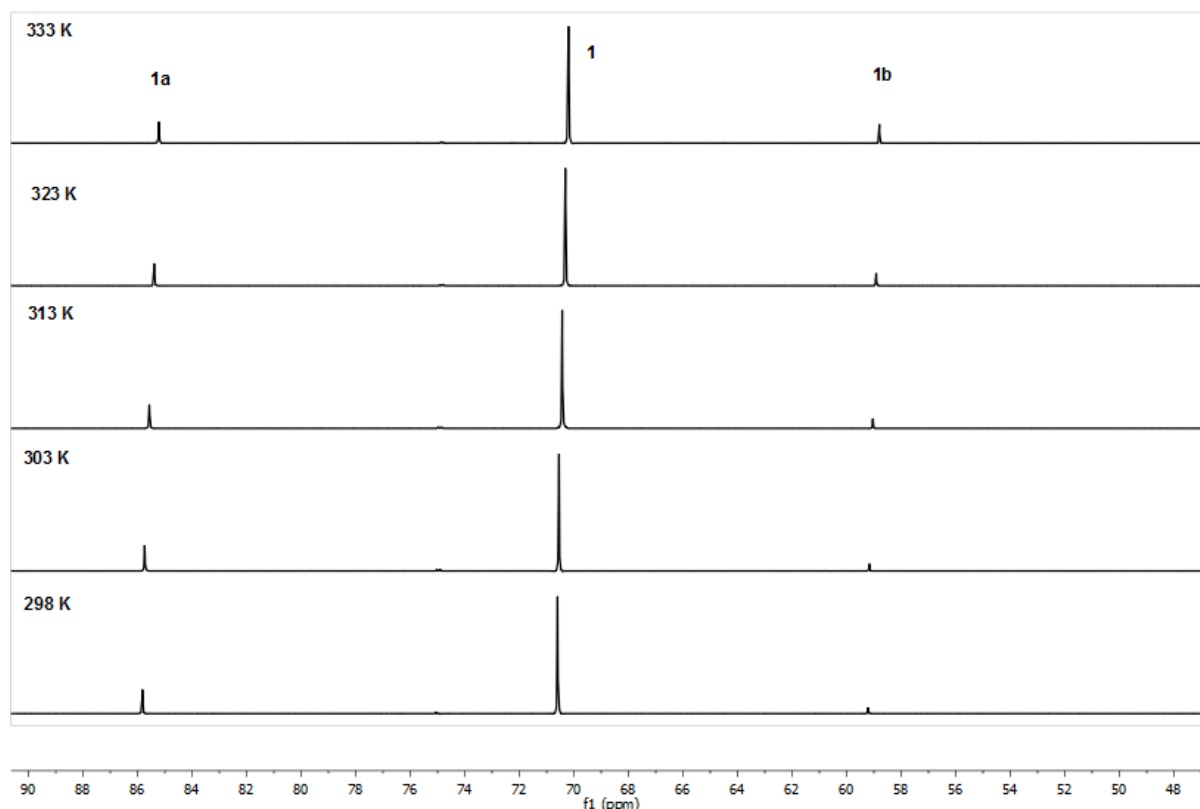


Figure 5. Stack plot showing results of variable-temperature $^{31}\text{P}\{^1\text{H}\}$ NMR spectra of the reduction of $[\text{Cp}^*\text{Fe}(\text{dmpe})(\text{CO})]^+[\text{BARf}_{24}]^-$ with 1 equivalent of $\text{Na}[\text{Et}_3\text{BH}]$ in THF, showing resonances attributable to starting **1**, **1a** and **1b** products. **1b** is favoured at elevated temperatures.

Variable-temperature ^{31}P NMR spectroscopy of a mixture of **1** and $\text{Na}[\text{Et}_3\text{BH}]$ (1:1 in THF) showed that the relative concentrations of each species (**1**, **1a** and **1b**) were actually temperature dependent and reversible, hence the composition was in equilibrium (Figure 5). While the concentration of **1** remains fairly constant with heating (298 – 333 K; see SI), **1a** is converted to **1b** (see Table S1 in SI). Since complete hydride delivery to **1**, and hence full conversion to **1a**, was never observed under these conditions, it is likely that this equilibrium involves $\text{Et}_3\text{B}/[\text{Et}_3\text{BH}]^-$ and thus implies that $[\text{Et}_3\text{BH}]^-$, **1a** and **1b** have comparable H^- donor strengths. Attempts to increase the conversion of **1** to reduced products using large excesses (> 10 eq.) of $\text{Na}[\text{Et}_3\text{BH}]$ did substantially increase the ratio of (**1a** + **1b**) : **1**, yet even under such conditions it was not possible to fully reduce all of the starting carbonyl compound. In these reactions it was noticed that as $\text{Na}[\text{Et}_3\text{BH}]$ was added (starting material resolved as a broad resonance in the ^{11}B NMR spectrum at $\delta \sim -12$ ppm) the ^{11}B NMR resonance moved proportionately downfield, dependent upon the initial amount of $\text{Na}[\text{Et}_3\text{BH}]$. This behaviour indicates formation of the bridging borohydride species $\text{Na}[\text{Et}_3\text{B}-\text{H}-\text{BEt}_3]$ (^{11}B : $\delta = 9.1$ ppm)[21] from liberation of Et_3B after initial H^- transfer, followed by interaction with $[\text{Et}_3\text{BH}]^-$; the latter is a poorer hydride donor which presumably hampers formation of **1a/1b** as it sequesters the more potent $\text{Na}[\text{Et}_3\text{BH}]$. Nevertheless, a protocol whereby **1** is fully converted was achieved by using a large excess of NaH in the presence of Et_3B to form $\text{Na}[\text{Et}_3\text{BH}]$ *in situ* at room temperature,[22] a combination which ensures that no free Et_3B (and hence no $\text{Na}[\text{Et}_3\text{B}-\text{H}-\text{BEt}_3]$) can form. Under these conditions the only borohydride reductant in solution is $\text{Na}[\text{Et}_3\text{BH}]$ (^{11}B : $\delta = -11.7$ ppm), and the equilibrium is concomitantly forced to one side, with **1b** the exclusive ^{31}P -containing product. A broad singlet at $\delta = -1.5$ ppm, also visible in the ^{11}B NMR spectra (alongside than that for the

[BArF₂₄] anion; see SI) of these reactions, was attributed to the presence of Na[Et₃B(OH)] (¹¹B: $\delta = -0.6$ ppm in C₆D₆)[23]. This borate species likely forms from the reaction of Et₃B with NaOH impurity in commercial samples of NaH.

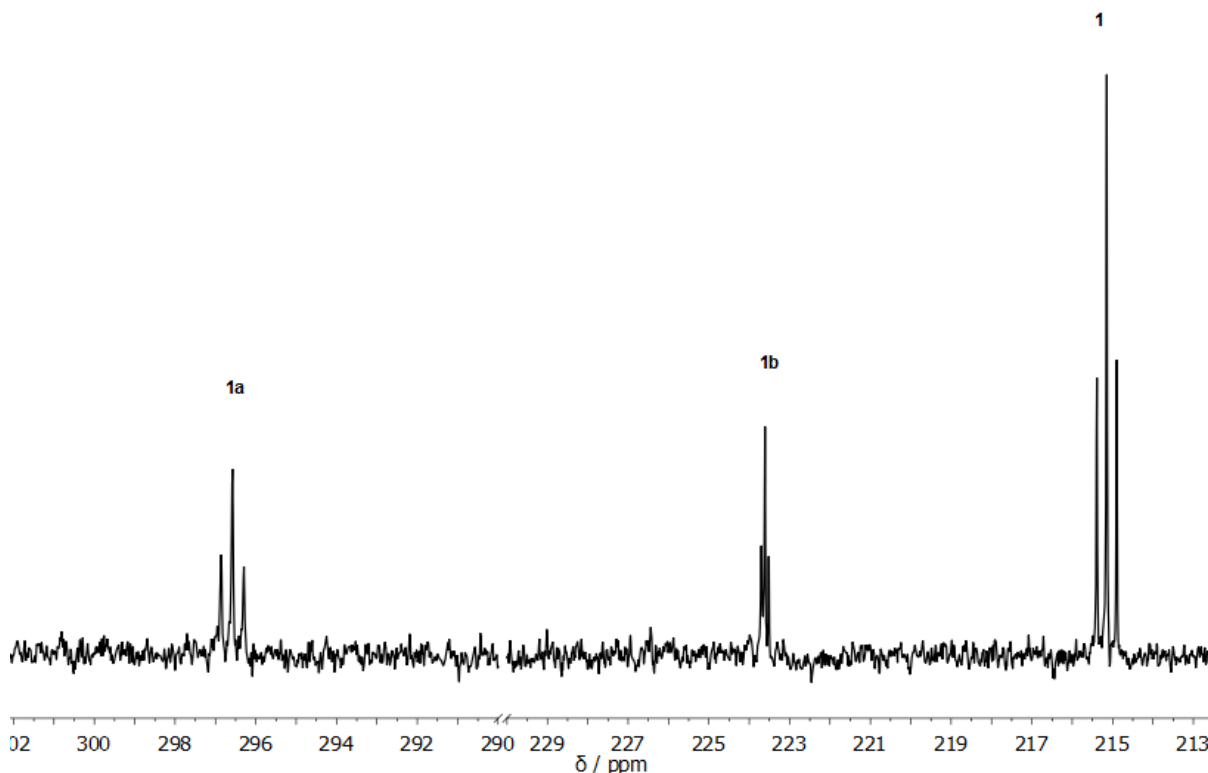


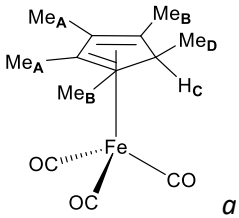
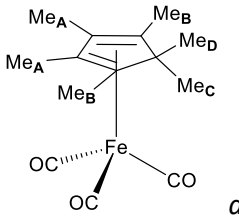
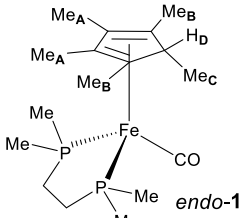
Figure 6. ¹³C{¹H} NMR spectrum of the reduction of ¹³CO-enriched **1** with 1 equivalent of Na[Et₃BH] in THF. New species **1a** and **1b** give rise to triplets at 296 ppm and 223 ppm, respectively.

Unfortunately, although **1b** could be obtained as the only ³¹P-containing species in these reactions, attempts to further purify this compound via crystallisation led only to **1** being isolated. In order to obtain additional spectroscopic information on the structural formulation of **1b**, a solution of **1** was irradiated with UV light (254 nm) under a ¹³CO atmosphere, which led to partial ¹³C isotopic enrichment of the CO ligand. Subsequent reduction of this labelled sample of **1** using Na[Et₃BH] (1 eq.) resulted in a mixture of **1**, **1a** and **1b** with attendant ¹³C {¹H} NMR shifts being readily observable for species undergoing a change to the ¹³CO ligand due to reduction. In addition to the resonance for **1**-¹³CO (¹³C: $\delta = 215$ ppm), two new downfield triplet resonances at 223 and 296 ppm were also observed (Figure 6). Further NMR experiments (HMBC; ¹³C-¹H and ³¹P-¹H) demonstrated a correlation between the signal at ¹³C $\delta = 296$ ppm and the diagnostic *CHO* resonance in the ¹H NMR spectrum, which also related to the ³¹P{¹H} resonance at $\delta = 85.4$ ppm; accordingly these shifts correspond to the formyl complex **1a**. Notably, the strongly downfield ¹³C NMR resonance in **1a** agrees very well with that previously reported for Cp*Fe(*n*Bu₃P)(CO)(CHO) ($\delta = 306$ ppm).[9]

By a process of elimination, the ¹³C NMR shift of $\delta = 223$ ppm strongly suggests that the CO ligand remains intact within species **1b**. Furthermore, the possibility that **1b** contains a -CH₂O- functional group may be confidently ruled out, since the ¹³C NMR resonance for such a moiety would be expected to appear at *ca.* 90 ppm, as exemplified by an oxymethylene Re species derived from the reductive coupling of CO ligands, after initial hydride ion reduction.[24] An alternative structure

might derive from H^- attack upon the Cp^* ring, which has been reported for the analogous (albeit less bulky and less electron-rich) $[\text{CpFe}(\text{dppe})(\text{CO})]^+$ system; this would force partial decoordination of the Cp^* ligand and form $(\eta^4\text{-C}_5\text{Me}_5\text{H})\text{Fe}(\text{dmpe})(\text{CO})$, in order to retain an 18-valence electron count for the Fe centre.[25] Spectroscopic evidence corroborating the latter as the identity of **1b** stems from the ^1H NMR spectrum of the reaction of **1** with Et_3B and excess NaH (see Table 3 and Figure 7): a quartet (1H; $\delta = 2.77$ ppm, $^3J_{\text{HH}} = 6.3$ Hz), doublet (6H; $\delta = 2.05$ ppm, $^4J_{\text{HH}} = 2.6$ Hz), doublet (3H; $\delta = 1.21$ ppm, $^3J_{\text{HH}} = 6.3$ Hz) and singlet (6H; $\delta = 1.10$ ppm) resonances clearly show a breaking of the symmetry of the Cp^* unit concomitant with addition of H^- , which is consistent with an $\eta^4\text{-C}_5\text{Me}_5\text{H}$ formulation. Furthermore, the protons for the Me peaks at $\delta = 1.10$ ppm in the $\eta^4\text{-C}_5\text{Me}_5\text{H}$ ligand demonstrate a long-range correlation to the ^{31}P resonance at $\delta = 58.6$ ppm assigned to **1b**, (by $^1\text{H}\text{-}^{31}\text{P}$ HMBC NMR spectroscopy) supporting the fact that the dmpe and $\eta^4\text{-C}_5\text{Me}_5\text{H}$ ligands are coordinated to the same Fe centre.

Table 3. ^1H NMR resonances for $(\text{exo-}\eta^4\text{-C}_5\text{Me}_5\text{H})\text{Fe}(\text{CO})_3$, $(\eta^4\text{-C}_5\text{Me}_6)\text{Fe}(\text{CO})_3$ and *endo-1b*.

| ^1H NMR label | Compound | | |
|------------------------|--|--|--|
| |  |  |  |
| Me _A | 1.26 | 1.08 | 1.10 |
| Me _B | 1.73 | 1.77 | 2.05 |
| H _c | 2.52 | - | - |
| Me _c | - | 1.21 | 1.21 |
| H _D | - | - | 2.77 |
| Me _D | 0.27 | 0.43 | - |

a Recorded in C_6D_6 , see reference 26. *b* Recorded in $\text{THF-}d_8$.

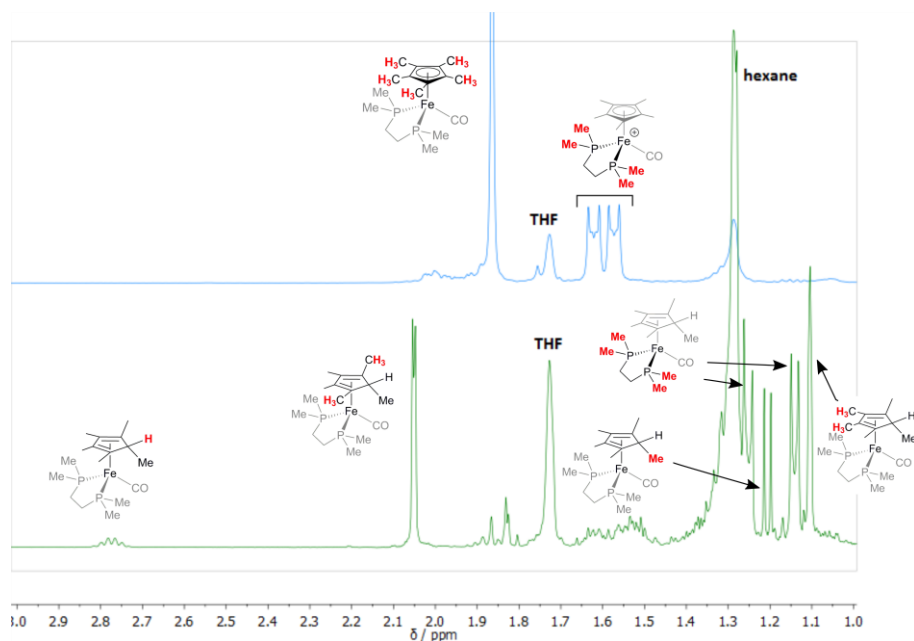
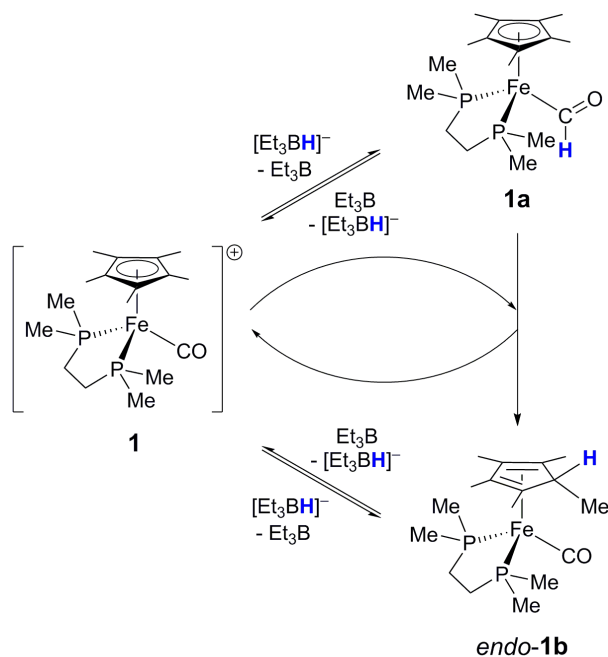


Figure 7. ^1H NMR spectra obtained for (a) starting material **1** ($\text{THF-}d_8$); (b) reaction of **1** with Et_3B and excess NaH ($\text{THF-}d_8$), which is proposed to form (*endo*- $\eta^4\text{-C}_5\text{Me}_5\text{H}$) $\text{Fe}(\text{dmpe})(\text{CO})$ (*endo*-**1b**).

Two stereoisomers are possible for compound **1b**. If hydride attack occurs to the least hindered face of the Cp^* ligand in **1** then this would force the Me group bound to the same C atom towards the most hindered side (forming *endo*-**1b**); conversely hydride attack to the face coordinated to the Fe centre would yield *exo*-**1b**, where the Me group points away from the Fe atom. Notably, the ^1H NMR signals for the previously reported species (*exo*- $\eta^4\text{-C}_5\text{Me}_5\text{H}$) $\text{Fe}(\text{CO})_3$ and ($\eta^4\text{-C}_5\text{Me}_6$) $\text{Fe}(\text{CO})_3$ bear a strong resemblance to those observed for **1b**, (see Table 3) except for demonstrating considerably more shielded environments for the MeCH protons (Me_D : $\delta = 0.27$ and 0.43 ppm, respectively)[27] when this group points away from the metal centre. In these instances, the CH_3 is directed towards the uncoordinated face of the ring π -system, which results in a diagnostically pronounced upfield shift, due to the magnetic anisotropy. Since the corresponding resonance for the Me group in **1b** is observed at an unremarkable δ value in its ^1H NMR spectrum, it may be concluded that the isomer formed under these conditions is actually the more hindered product *endo*-**1b**. [28]



Scheme 4. Partial reduction of **1** with Na[Et₃BH] provides three possible compounds: formyl **1a** and *endo*-**1b**. Since Et₃B, **1**, **1a** and **1b** have similar hydride ion affinities, all species are in equilibrium, with Et₃B acting as a hydride shuttle between **1**, **1a** and *exo*-**1b**.

A possible mechanism for the formation of *endo*-**1b**, which is expected to be the least stable product of the *endo/exo*-pair, is shown in Scheme 4. Initial delivery of hydride from [Et₃BH]⁻ can occur to either the CO ligand (affording **1a**) or the Cp* ligand from the top face (affording *endo*-**1b**), and liberating free Et₃B. Since **1**, **1a** and *endo*-**1b** are in mutual equilibrium and therefore have similar hydride anion affinities, it is plausible that **1a** can act as a hydride donor (from the CHO moiety) to **1**, which would also be expected to be delivered to the least hindered face of the Cp* ring, hence providing an alternative route to *endo*-**1b**. The interconversions are mediated by Et₃B, which acts as a hydride shuttle between the species. When excess NaH is employed all Et₃B is converted to Na[Et₃BH], which increases the reducing power of the medium and shifts the equilibrium completely to *endo*-**1b** (which is presumably the most difficult species to form on account of its high electron density and dearomatized Cp* unit, in comparison with **1a**), and shuts down the H⁻ shuttling mechanism for interconverting the species.

Conclusions

A cationic monocarbonyl complex [Cp*Fe(dmpe)(CO)]⁺ has been prepared as its [BArF₂₄]⁻ salt (**1**), using a simple methodology, in order to investigate its reactivity with hydride sources. The compound has been spectroscopically characterised and structurally elucidated in the solid-state; the highly electron-rich nature of the metal centre imparted by the strongly donating Cp* and dmpe ligands is reflected in a much lower C-O stretching frequency in comparison to similar Fe compounds which have previously served as precursors to formyl complexes. The potent hydride transfer agent Na[Et₃BH] was required to effect reduction of the CO ligand and yield Cp*Fe(dmpe)(CHO) (**1a**), which is in equilibrium with a structural isomer wherein the hydride attacks the Cp* ligand instead – (η⁴-C₅Me₅H)Fe(dmpe)(CO) (*endo*-**1b**) – and starting **1**. Hydride shuttling between **1**, **1a** and **1b** appears to be facilitated by Et₃B, showing all reduced Fe species to be potent hydride donors in their own right.

Remarkably, these mixtures are stable to heating (333 K), demonstrating **1a** to be one of the most thermally robust formyl compounds known. Further reactivity studies of formyl species, and their potential application in homogeneous CO hydrogenation, are currently underway in our laboratory.

Acknowledgements

We thank BP plc and the EPSRC for generous financial support of a PhD (S. J. G.; Industrial CASE studentship award, voucher no. 12220535) and the Royal Society for a University Research Fellowship (AEA; UF/160395).

References

- [1] N.M. West, A.J.M. Miller, J.A. Labinger, J.E. Bercaw, *Coord. Chem. Rev.* 255 (2011) 881–898.
- [2] C.K. Rofer-DePoorter, *Chem. Rev.* 81 (1981) 447–474.
- [3] M.D. Farnos, B.A. Woods, B.B. Wayland, *J. Am. Chem. Soc.* 108 (1986) 3659–3663.
- [4] S.L. Van Voorhees, B.B. Wayland, *Organometallics*. 6 (1987) 204–206.
- [5] P.J. Fagan, K.G. Moloy, T.J. Marks, *J. Am. Chem. Soc.* 103 (1981) 6959–6962.
- [6] P.A. Belmonte, F.G.N. Cloke, R.R. Schrock, *J. Am. Chem. Soc.* 105 (1983) 2643–2650.
- [7] J.A. Gladysz, *Adv. Organomet. Chem.* 20 (1982) 1–38.
- [8] K.R. Lane, L. Sallans, R.R. Squires, *Organometallics*. 4 (1985) 408–410.
- [9] C. Lapinte, D. Catheline, D. Astruc, *Organometallics*. 7 (1988) 1683–1691.
- [10] S.G. Davies, J. Hibberd, S.J. Simpson, *J. Chem. Soc., Chem. Commun.* (1982) 1404–1405.
- [11] S.G. Davies, S.J. Simpson, *J. Organomet. Chem.* 268 (1984) C53–C55.
- [12] P.J. Hill, L.R. Doyle, A.D. Crawford, W.K. Myers, A.E. Ashley, *J. Am. Chem. Soc.* 138 (2016) 13521–13524.
- [13] A.D. Piascik, R. Li, H.J. Wilkinson, J.C. Green, A.E. Ashley, *J. Am. Chem. Soc.* 140 (2018) 10691–10694.
- [14] L.R. Doyle, A. Heath, C.H. Low, A.E. Ashley, *Adv. Synth. Catal.* 356 (2014) 603–608.
- [15] Z. Teixeira, S.P. Vasconcellos, L. Koike, G.H.M. Dias, *Quim. Nov.* 30 (2007) 494–496.
- [16] O. V Dolomanov, L.J. Bourhis, R.J. Gildea, J.A.K. Howard, H. Puschmann, *J. Appl. Crystallogr.* 42 (2009) 339–341.
- [17] L.J. Bourhis, O. V Dolomanov, R.J. Gildea, J.A.K. Howard, H. Puschmann, *Acta Crystallogr. A* 71 (2015) 59–75.
- [18] G.M. Sheldrick, *Acta Crystallogr. C* 71 (2015) 3–8.
- [19] A. de la J. Leal, M.J. Tenorio, M.C. Puerta, P. Valerga, *Organometallics*. 14 (1995) 3839–3847.
- [20] D. Catheline, D. Astruc, *J. Organomet. Chem.* 226 (1982) C52–C54.
- [21] H. Li, A.J.A. Aquino, D.B. Cordes, F. Hung-Low, W.L. Hase, C. Krempner, *J. Am. Chem. Soc.* 135 (2013) 16066–16069.
- [22] J.B. Honeycutt, J.M. Riddle, *J. Am. Chem. Soc.* 83 (1961) 369–373.

- [23] R. Koester, G. Seidel, B. Wrackmeyer, Chem. Ber. 125 (1992) 617–625.
- [24] A.J.M. Miller, J.A. Labinger, J.E. Bercaw, J. Am. Chem. Soc. 130 (2008) 11874–11875.
- [25] S.G. Davies, S.D. Moon, S.J. Simpson, S.E. Thomas, J. Chem. Soc., Dalt. Trans. (1983) 1805–1806.
- [26] C. Zou, M.S. Wrighton, J.P. Blaha, Organometallics. 6 (1987) 1452-1458
- [27] ¹H NOESY experiments were also performed to obtain additional evidence for whether **1b** exists as the *endo*- or *exo*-isomer. Unfortunately, the results were inconclusive and it was not possible to confirm which isomer corresponds to **1b**, when it is formed under conditions of excess NaH.
- [28] P. V. Balakrishnan, P.M. Maitlis, J. Chem. Soc. A Inorganic, Phys. Theor. (1971) 1712-1715.